Journal of Alloys and Compounds 1039 (2025) 182787

Contents lists available at ScienceDirect

Journal of Alloys and Compounds

journal homepage: www.elsevier.com/locate/jalcom

Research article

Evolution at the nanoscale of magnetic clustering of the Griffiths-like phase in $Tb_{4.925}La_{0.075}Si_2Ge_2$

N. Marcano [a,*], E.M. Jefremovas [b,c], I. Titov [c], A. Michels [c], N.J. Steinke [d], J.H. Belo [e], J.P. Araújo [e], P.A. Algarabel [f,g], L. Fernández Barquín [a]

[a] Departamento CITIMAC, Facultad de Ciencias, 39005, Santander, Spain
[b] Institute of Physics, Johannes Gutenberg University of Mainz, 55128, Mainz, Germany
[c] Department of Physics and Materials Science, University of Luxembourg, 1511, Luxembourg, Luxembourg
[d] Institut Laue-Langevin, 71 Avenue des Martyrs CS 20156 CEDEX 9, 38042, Grenoble, France
[e] IFIMUP, Departamento de Física e Astronomia, Facultad de Ciencias, Rua do Campo Alegre s/n, 4169-007, Porto, Portugal
[f] Instituto de Nanociencia y Materiales de Aragón (INMA), CSIC-Universidad de Zaragoza, 50009, Zaragoza, Spain
[g] Departamento de Física de la Materia Condensada, Universidad de Zaragoza, 50009, Zaragoza, Spain

ARTICLE INFO

Keywords:
Rare earth alloys
Griffiths-like phase
Small angle neutron scattering
Cluster-spin glass
Ageing

ABSTRACT

Griffiths-like phases (GP) are connected to disordered magnetic nanostructures. Here, we focus on the Giant Magnetocaloric compound $Tb_{5-x}La_xSi_2Ge_2$ with $x = 0.075$ where a re-entrant cluster-glass state (CGS) emerges at a characteristic freezing temperature $T_F \sim 140$ K within the GP (110–180 K), i.e. above the Curie temperature (T_C). This unconventional magnetic state has been studied via temperature-dependent DC magnetization (5–300 K), time-dependent macroscopic AC susceptibility (80–200 K), including ageing and memory experiments, and magnetic small-angle neutron scattering (SANS), above T_C (110–250 K). This approach allows to reveal the microscopic structure of the GP at the nanoscale in this system. AC susceptibility and DC magnetization confirm the presence of interacting short-range (< 2 nm) ferromagnetic (FM) clusters in the GP. The Langevin-like field dependence of the isothermal magnetization provides a quantitative assessment of the temperature dependence of the cluster size. Memory effects and ageing phenomena within GP are indicative of magnetically-frustrated states. Our results reveal that the dynamics is affected by the progressive coupling among CGS and GP towards the FM state. SANS correlation lengths between 1-5 nm above T_F are determined from the calculated magnetic correlation function *C(r)*, which is computed from the magnetic SANS intensity. A phenomenological model based on the formation of FM clusters with intercluster (FM) interactions within a PM matrix is proposed to explain the unusual re-entrant glassy behaviour in the PM state. These findings serve as another experimental reference for the global understanding of disordered magnetic compounds.

1. Introduction

Understanding the role of magnetic disorder in condensed matter physics is a growing research area that has gained significant importance in recent decades (see, *e.g.*, Ref. [1]). Magnetic disorder can manifest in a variety of forms in magnetic materials. The most investigated is that of isolated spins in a metallic crystalline matrix in archetypal canonical spin glasses, showing a freezing transition [2]. The very diluted magnetic state is a source for such frustrated states, which are quantitatively evaluated through the values of critical exponents extracted at the freezing temperature [3,4]. When the magnetic concentration in the alloy is increased, correlations among the spins are triggered, building up a more collective cluster-glass phase [5–8].

On top of the described canonical spin glasses, caused by the frustration of the Ruderman–Kittel–Kasuya–Yosida (RKKY) interactions, one can investigate the magnetic phenomena that arise when the crystalline and magnetic structures couple. This is the case of the Griffiths-like phases (GP), which is characterized by the presence of subtle magnetic order at some temperature T_G above the Curie temperature, *i.e.*, within the paramagnetic state. In this situation, adjacent magnetic clusters interact at first neighbour range, increasing in size and number while approaching the magnetic order. The GP therefore becomes the seed for magnetic order in some systems [9,10]. Moreover, the notion of GP phases is also connected to basic electronic phenomena, alternatively found at very low temperatures in strongly correlated systems [11].

* Corresponding author.
E-mail address: marcanon@unican.es (N. Marcano).

https://doi.org/10.1016/j.jallcom.2025.182787
Received 25 April 2025; Received in revised form 1 August 2025; Accepted 3 August 2025
Available online 16 August 2025

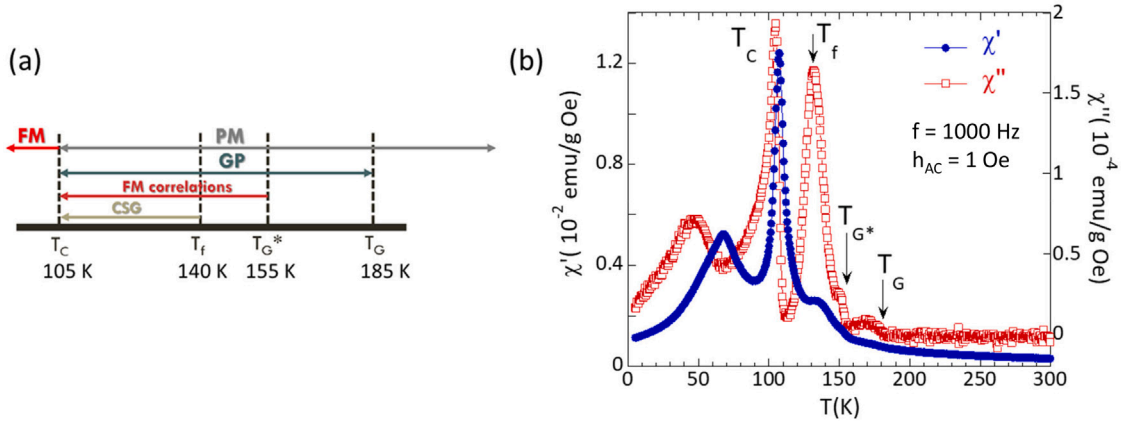

Fig. 1. (Colour online) (a) A sketch (linear phase diagram) indicating the different temperature-dependent regions of interest of the alloy (Griffiths-like phase, cluster-spin glass (CSG), ferromagnetic). (b) In-phase($\chi'(T)$) and out-of-phase ($\chi''(T)$) components of the AC susceptibility as a function of temperature of $Tb_{4.925}La_{0.075}Si_2Ge_2$ measured at 1000 Hz and in an applied AC field of h_{AC} = 1 Oe in the temperature range 5–300 K.

All the evidences just described support the spell of GP in the quest of deepening into fundamental physics. Moreoever, the existence of GP has been shown in a limited number of materials but with a high technological potential. These include transition metal oxides [12–16], magnetic semiconductors [17,18], quantum magnetic systems [19,20], multiferroics [21,22] and transition metal based Heusler alloys [23–26].

Intermetallic systems, such as the $R_5(Si_yGe_{1-y})_4$ type (hereafter 5:4 system) with R = Gd, Tb, Dy or Ho [27–29] display GP as well, on top of their notable performance in magnetocaloric applications. This 5:4 family constitute an interesting class of materials exhibiting multifunctional properties such as colossal magnetrostriction, giant magnetoresistance (GMR), giant magnetocaloric (GMC) effect, spontaneous generation of voltage [29] and negative thermal expansion [30]. Nowadays, the potential application of these alloys in energy saving devices speaks by itself on the importance of the study of these alloys [31]. The physical properties of these 5:4 family are strongly determined by their complex layered crystallographic structure, which is built by the stacking of rigid two-dimensional layers (slabs) via partially covalent interslab Si(Ge)-Si(Ge) bonds [32]. Further details on the crystallographic structure can be found in [29].

The presence of the GP within the 5:4 family was first reported in $Tb_5Si_2Ge_2$ [27]. Small-angle neutron scattering (SANS) experiments revealed the formation of nanometric regions, ferromagnetically coupled in the PM regime (sporting a spin-spin correlation length $\xi \sim 0.5$–8 nm) below T_G = 200 K, well above T_C = 110 K [27]. These small clusters give rise to the characteristic downward deviation of the reciprocal susceptibility $\chi_{DC}^{-1}(T)$ from the standard Curie–Weiss prediction below T_G, representing the fingerprint of a GP. According to further studies by Pereira et al. the formation/rupture of the interslab Si(Ge)-Si(Ge) bonds is the key component in understanding the appearance of the GP in these 5:4 systems [28].

Chemical substitution is a very suitable strategy to alter the GP phase, as it modifies the distance and chemical bonding between the slabs. This can be achieved either by tuning the Si/Ge doping or by exchanging the R ions $R_{5-x}R_{x'}(Si_yGe_{(1-y)})_4$ [29]. In this context, Belo et al. reported a comprehensive study on the structural and magnetic properties of the $Tb_{5-x}La_xSi_2Ge_2$ explaining the role of nonmagnetic atoms (La) on parent compounds exhibiting a spontaneous magneto-structural transition and on how it affects the magnetic exchange mechanism [33]. Inspired by this work, Marcano et al. carried out a thorough magnetic study understanding the role of La on the mechanism responsible for the formation of the short-range FM clusters in the GP in the parent compound, $Tb_5Si_2Ge_2$ [34]. Interestingly, a non-reported cluster-glass state within the GP in the x = 0.075 compound was observed. Once the Griffiths-like phase was established ($T < T_G$ = 185 K) i.e, in the paramagnetic regime, ferromagnetic-like correlations were built up at around $T_{G^*} \sim 155$ K, and became frozen at a lower temperature $T_F \sim 140$ K [34], resembling a re-entrant spin glass behaviour. To aid in understanding and visualize the complex magnetic behaviour of the x = 0.075 compound, we present a simple sketch (linear phase diagram) that illustrates the different temperature-dependent regions of interest such as Griffiths-like phase, cluster-spin glass (CSG) and ferromagnetic phases (Fig. 1(a)) according to [34].

It is worth mentioning that in a re-entrant spin glass state the magnetic moments become cooperatively coupled at the phase ordering transition and a long-range ferromagnetic order is clearly established. However, the presence of magnetic clusters (small domains) favours the appearance of a freezing at lower temperatures with a concomitant increase of the anisotropy and reduction of magnetization [35]. In the case of x = 0.075, this process occurs at higher temperatures than the ferromagnetic conventional ordering, precisely in the GP. This unusual re-entrant behaviour in the GP state, was not detected in the non-diluted compound $Tb_5Si_2Ge_2$ (x = 0) since the magnetic signal coming from the short-range FM clusters in the GP was much weaker. Such drastic weakening of the magnetic response of the GP clusters over the PM matrix could be connected to a smaller cluster size and/or a smaller number of clusters in the non-diluted compound relative to the diluted compound, x = 0.075. These findings reveal that these $Tb_{5-x}La_xSi_2Ge_2$ alloys with minute La-substitutions constitute a unique playground to unveil the relation of magnetic disorder with the percolation of GP-like clusters and the mechanism of the cluster glass state.

In this work, we employ DC-magnetization to determine the magnetic state, and AC susceptibility to determine the freezing dynamics and memory effects (ageing) in x = 0.075 compound. By evaluating the time-dependent magnetic susceptibility response we access the very subtle dynamic responses associated to the GP clusters. The isothermal *M(H)* curves provide information about the size and concentration of the GP magnetic clusters within the paramagnetic matrix and its evolution with temperature. To determine the correlations among clusters, we employ small-angle neutron scattering (SANS). This technique allows to extend the study at the magnetic nanoscale to disclose the size of the GP clusters and to establish the magnetic correlation lengths among these randomly arranged entities.

2. Experimental

The polycrystalline $Tb_{5-x}La_xSi_2Ge_2$ samples with x = 0.075 were prepared using an arc-melting furnace. The starting elements were

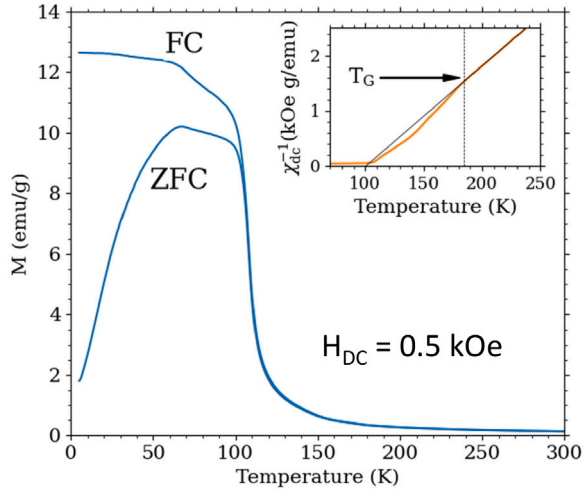

Fig. 2. (Colour online) ZFC-FC magnetization of $Tb_{4.925}La_{0.075}Si_2Ge_2$ as a function of temperature measured in an applied DC field of $H_{DC} = 0.5$ kOe.

99.99 wt% pure Tb, 99.9 wt% pure La, and 99.9999 wt% pure Si and Ge (from Alfa Aesar). The quality of the as-cast samples was checked by room-temperature x-ray diffraction and scanning electron microscopy measurements. Further details on the sample preparation and basic structural characterization at room temperature can be found in Refs. [27,33]. The magnetic characterization was carried out by means of static DC magnetization and dynamic AC susceptibility $\chi_{AC}(T,t)$ measurements in a QD-MPMS (SQUID) magnetometer located at the University of Cantabria. DC magnetization measurements were performed under applied magnetic fields H_{DC} = 0.5 kOe and within a temperature range of 5 to 300 K (including a set of M(H) curves). Both in-phase $\chi'_{AC}(T)$ and out-of-phase $\chi''_{AC}(T)$ components of the linear susceptibility were recorded using an oscillating magnetic field amplitude of h_{AC} = 1 Oe and an AC frequency of f = 1000 Hz. To probe memory effects and ageing phenomena we have recorded the out-of-phase χ'' component of the dynamic AC susceptibility (χ_{AC}) between 80–200 K under an oscillating magnetic field amplitude of 3.13 Oe and a frequency of f = 0.2 Hz. Several protocols can be used to probe such time-dependent phenomena [36–40]. In this work, we have mimicked the one described in [41], where memory effects are probed by tracing the difference between the out-of-phase $\chi''_{AC}(T)$ measured upon warming, having cooled down the sample following two protocols. First, the sample is cooled down without making any pause. Then, the sample is measured upon warming ($\chi''_{ref}(T)$). Second, the sample is cooled sequentially, making three stops while cooling down at T_W = 90, 116, and 145 K for t > 104 s. During this time, the system gets aged, and a particular spin disorder configuration can be established. Then, once the cooling is resumed, the sample is measured upon warming in the same manner as for $\chi''_{ref}(T)$. This establishes the $\chi''_{warming}(T)$ curve. If memory effects are to be evidenced, a drop in the $\chi''_{warming}(T)$ just before T_W will be observed. The SANS measurements were performed at the D33 instrument located at the Institut Laue-Langevin, France. We used an average incident neutron wavelength of λ = 4.6 Å with a wavelength broadening of $\Delta\lambda/\lambda$ = 10 % (FWHM). Three sample-to-detector distances (2.3, 7.8, and 12.8 m) were selected in order to cover a wide range of scattering vectors (0.035 $nm^{-1} < q <$ 2.6 nm^{-1}). SANS data were taken at several temperatures between 90 and 250 K. A SANS run in the paramagnetic temperature regime (at 250 K, above T_G) was taken as the nuclear (structural) background contribution and was subtracted from the SANS patterns at lower temperatures to derive the magnetic signal.

3. Results and discussion

3.1. Macroscopic magnetic characterization

Fig. 1(b) shows the different magnetic states in the compound x = 0.075. It shows the in-phase ($\chi'(T)$) and out-of-phase ($\chi''(T)$) components of the AC magnetic susceptibility as a function of temperature recorded at a single AC frequency f = 1000 Hz without DC magnetic field. Starting at low temperatures with the long-range ordered state, a pronounced cusp at $T_C \sim 105$ (1) K in both $\chi'(T)$ and $\chi''(T)$ stands out as a clear sign of the FM phase transition. The nature of the anomaly observed in $\chi'(T)$ at $T_{SR} \sim 65$ K is assigned to a spin reorientation process occurring within the long-range ferromagnetic phase, similar to that observed and thoroughly studied in the parent compound $Tb_5Si_2Ge_2$ [42–44]. The out-of-phase component $\chi''(T)$ highlights the distinct magnetic regimes present in this system while in the paramagnetic state: The slight anomaly at $T_G \sim 185$ K marks the emergence of short-range magnetic clusters within the paramagnetic state, signifying the onset of the Griffiths-like phase (GP). Meanwhile, the peak observed at $T_{G^*} \sim 155$ K indicates that ferromagnetic-like correlations are developing among the GP clusters. At lower temperatures, the peak at $T_F \sim 140$ K is linked to the freezing of these clusters, in a Cluster-Spin Glass (CSG) fashion, which occurs following a strict critical slowing down process according to previous studies [34]. Finally, the peak observed at 50 K corresponds to the spin reorientation process. The fact that the peak in the imaginary component $\chi''(T)$ is shifted to lower temperatures compared to $\chi'(T)$ is a common feature related to the phasing in AC-susceptibility measurements [35].

The zero-field-cooled (ZFC) and field-cooled (FC) static DC-magnetization curves at a relatively low applied field H_{DC} = 0.5 kOe are presented in Fig. 2. In the FC protocol, the sample is cooled to 5 K in the presence of the measuring field and the magnetization is recorded in a heating run keeping the field constant. In the ZFC protocol the sample is cooled down to 5 K in zero field (magnet quenched) and then, the measuring field is applied and the magnetization is recorded as a function of the temperature in the heating up run. The ferromagnetic transition (obtained by the minimum of the numerical derivative, dM/dT) occurs at T_C = 105(1) K, matching obviously the dynamic AC-measurements. Such a phase transition is preceded by the spin reorientation transition at T_{SR} = 65 K, during the ZFC measurements. The irreversibility observed between the ZFC and FC magnetization data below T_C is related, in general, to magnetic disorder. In long-range FM systems this is connected basically to domain wall pinning [42,43]. The large difference between ZFC and FC magnetization data reflects sizeable pinning effects in this compound. The inset of Fig. 2 shows the temperature dependence of the inverse of the magnetic susceptibility ($\chi^{-1}_{DC}(T)$) at 0.5 kOe. In this representation the onset of the Griffiths-like phase T_G is defined as the temperature where the deviation from the typical Curie–Weiss lineal behaviour is building up, according to the criteria established in the seminal work by Magen et al. [27]. Our earlier studies demonstrated the field dependence of the downward deviation from Curie–Weiss linear behaviour in $\chi^{-1}_{DC}(T)$, highlighting distinct sensitivities of the transitions associated with T_G and T_{G^*} to the applied magnetic field. In line with these observations, the steplike anomaly in $\chi^{-1}_{DC}(T)$ related to T_{G^*} becomes barely detectable at 0.5 kOe, while the deviation at T_G is smaller compared to that observed at lower fields. Notably, a relatively small magnetic field (1 kOe) is required to fully suppress the deviation in $\chi^{-1}_{DC}(T)$ at T_G [34].

To further investigate the formation of FM clusters in the GP along with its interactions, M(H) isotherms at different temperatures ($T > T_C$) have been investigated. Fig. 3(a) includes six M(H) curves at different temperatures between 110 K and 250 K. It is worth noting that Arrott Plots (M^2 versus H/M) from a previous study [34] revealed the absence of spontaneous magnetization above T_C (105 K), indicating the lack of long-range FM ordering above T_C. The linear M-H curve at T = 250 K is

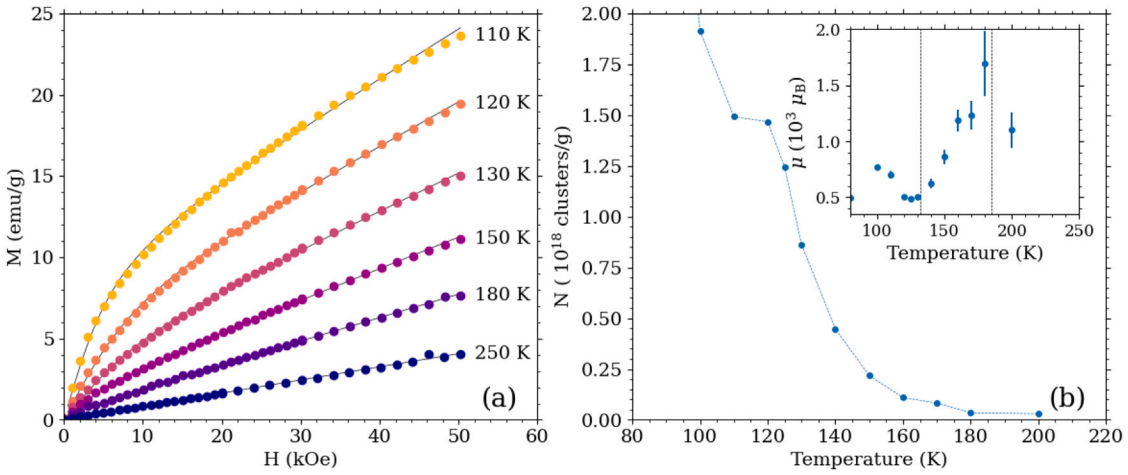

Fig. 3. (Colour online) (a) Isothermal magnetization curves M(H) of $Tb_{4.925}La_{0.075}$ Si_2Ge_2 for representative temperatures along with the fits (black solid line) to the Eq. (1) and to conventional PM behaviour (T = 250 K). (b) T- dependence of the number of clusters per unit mass (N) and the moment of the clusters (μ_B) extracted from the Langevin fitting of isotherms at different T within the GP (inset). Vertical dashed lines indicate T_F (140 K) and T_G (185 K) position.

easily interpreted on the base of a conventional PM behaviour (straight line in Fig. 3(a)) which becomes progressively nonlinear (curved) towards the temperature at which the true FM state is settled down. The nonlinear M-H curve for 120–200 K isotherms (well above T_C) however, suggest the presence of a dominant paramagnetic component coexisting with a weak ferromagnetic state. These results cannot be explained on the basis of conventional theories. Therefore, an analytical expression with a combination of two magnetic components has been employed to identify the magnetic interactions within the GP. The experimental curves for $T < 250$ K can be well described by assuming a modified Langevin function represented by

$$M(H) = N\mu[\coth(\mu H/k_B T) - k_B T/\mu H] + \chi H \quad (1)$$

Where N is the number of magnetic clusters per unit mass, μ is the average magnetic moment per cluster, and χ is the field-dependent Curie-type magnetic susceptibility [15,45,46]. Langevin fittings (continuous lines) to the 110–200 K isotherms are plotted in Figure 3(a). As shown in Fig. 3(a), magnetization data follows Eq. (1) in this temperature range. A similar approach following that presented in [47] has been taken into account to derive the parameters, where the change of regime in M(H) between low and high fields is relevant. In the present case, the value of χ at 200 K is $\chi \sim 0.12$ emu/g kOe, and increases up to $\chi \sim 0.24$ emu/g kOe when closing in T_C. From these fits, the magnetic cluster moment μ and number of clusters per unit of mass (N) can be obtained as a function of temperature (see Fig. 3(b)). Regarding the cluster magnetic moment, it can be observed that it progressively decreases from approximately 1600 μ_B at ~ 185 K (T_G), when the nucleation of FM clusters within the PM region occurs, down to approximately 450 μ_B at 120 K (just below T_F). With respect to N, the number of clusters per gram, it can be observed that it continuously increases as cooling from $N \sim 3.44 \times 10^{16}$ g^{-1} at 180 K down to $N \sim 1.47 \times 10^{18}$ g^{-1} at 120 K. According to these observations, as cooling down below T_G, the paramagnetic matrix breaks into an increasing number of clusters, whose size decreases as the freezing temperature T_F is approached. The observed anomalous temperature dependence of cluster size may be attributed to the presence of competing magnetic interactions and frustration in this temperature regime, in a manner analogous to the behaviour reported by Akram et al. in $Eu_{0.5}Sr_{0.5}MnO_3$-$EuMnO_3$ composites [46]. Below T_F, a slight increase in cluster size is observed upon further cooling, which can be attributed to the close proximity of T_C, potentially enhancing long-range correlations. Assuming the clusters have a spherical shape and using the effective paramagnetic moment (7.1 μ_B/Tb^{3+}) along with the unit cell volume (847.3 Å^3) [33] and the number of Tb^{3+} per unit cell (a total of 36 atoms per unit cell, 20 of which are Tb^{3+}) [48], it is possible to estimate the size (diameter) of these clusters. The value for the diameter of the cluster at T_G from this estimation is ~ 1.5 nm. It is worth to note that assessing the role of magnetic anisotropy with the competing exchange interactions in the presence of frustration as T_C is approached is not straightforward in this context. In particular, the applicability of the Langevin approach may be limited when attempting to accurately describe the Griffiths-like phase in our system. Nevertheless, the model still provides a useful framework to estimate, to some extent, the size of the magnetic clusters and its interactions. These estimations are further supported by (pretty unique in GP) Small-Angle Neutron Scattering (SANS) measurements, presented in a later section, which represent the most suitable technique for probing such features.

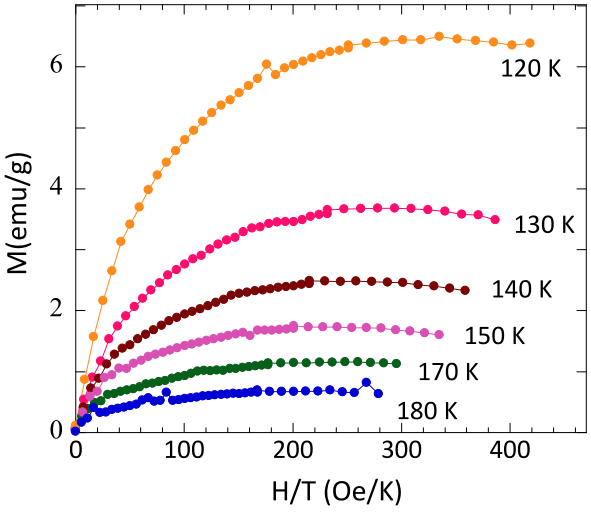

Fig. 4. (Colour online) Magnetization M versus H/T plots for representative temperatures in the GP regime $T_C < T < T_G$. The lines are intended as guides for the eye.

Considering the presence of ferromagnetic (FM) clusters of nanometric size in the Griffiths-like phase ($T > T_C$), one can examine the magnetic correlations among them. For this purpose, and according to Bean et al. [49] the magnetization M versus H/T has been displayed at different temperatures within the GP ($T_C < T < T_G$) in Fig. 4 (all the paramagnetic components were subtracted). If the clusters were superparamagnetic (i.e., they act like independent single domain nanoparticle entities), a scaling behaviour is expected and the curves

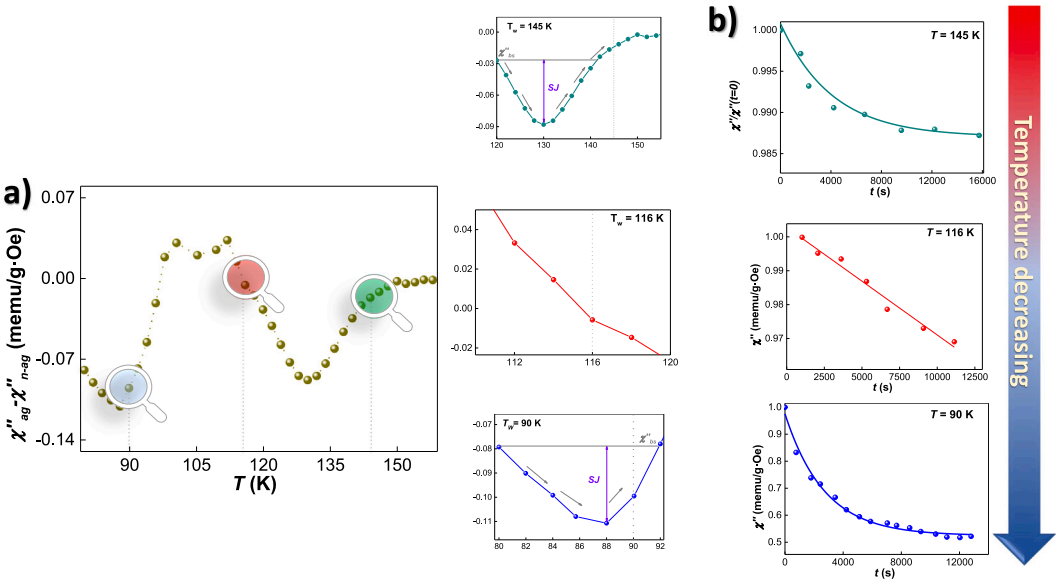

Fig. 5. (Colour online)(a) $\chi''_{ag} - \chi''_{n-ag}$ difference versus temperature. Note the Y-axis units (mili emu/g· Oe). The cooling has been arrested at T_W = 90, 116, and 145 K (marked with grey dashed lines), letting the system to be aged for t > 104 s. Memory effects are evidenced by the drop in the difference at $T < T_W$ at 90 and 145 K, quantified by means of the SJ parameter (marked in purple). (b) χ'' versus t evolution at the different T_W. As expected, only at 145 and 90 K, a slow out-of-equilibrium power-law with small exponent fits well the data.

would collapse onto a single one [15,49,50]. In the present case, the lack of superposition of these curves rules out the presence of superparamagnetism in the Griffiths phase, and magnetic intercluster interactions are definitely present. Small-Angle Neutron Scattering (SANS) will give more details (see section 3.3) on the nature of correlations of clusters.

3.2. Rejuvenation and ageing measurements

Being demonstrated the presence of GP in our sample, we have employed dynamic AC susceptibility to characterize the non equilibrium dynamics of our system. More precisely, ageing and rejuvenation phenomena, very similar to the one of Spin Glasses [6,36,41,51,52], have been investigated. Fig. 5 showcases the time-dependent out-of-phase χ'' component, measured as a function of (a) temperature (T), and (b) time (t). In Fig. 5(a), memory effects are easily detected by the observation of a drop at T_W = 145 K and 90 K, while no effects are retrieved at T_W = 116 K. Starting with such a T_W = 145 K ($T < T_G$), the occurrence of time-dependent phenomena can be understood as effects connected to the Griffiths regime, where short-range FM correlations achieve a parallel alignment of some magnetic Tb^{3+} moments, therefore building up magnetically-ordered clusters within the globally disordered state. Deepening in the analysis, we provide a quantification of such a disordered state by means of the Spin Glass rejuvenation jump SJ parameter [51] defined as:

$$SJ = \left| \frac{\chi''_{\text{memory}} - \chi''_{\text{bs}}}{\chi''_{\text{bs}}} \right| \quad (2)$$

where $\chi''_{memory} = \chi''_{ag} - \chi''_{n-ag}$, and χ''_{bs} is defined as the χ''_{memory} value corresponding to the temperature at which memory effects emerge (see grey line in right panel of Fig. 5(a)). Such a parameter enables the comparison of the memory effect robustness across various SGs systems. Our sytem exhibits SJ = 10.3, which is very similar to the one of canonical SGs, as CuMn (SJ = 7.5) and $CdCr_{1.7}In_{0.3}S_4$ (SJ = 12) [38,53], and remarkably larger than the one (around 0.5) quantified for the surface spin glass magnetic moments of Superantiferromagnetic $NdCu_2$ nanoparticles [51]. This should be connected to the fact that the size of the GP clusters contains a definite lower number of rare-earth moments. Although both SG and GP account for a slow non equilibrium dynamics, it is worth commenting on their differences. In this sense, the drop in χ'' (T) tends to be shifted downwards in GP with respect to SG. In this sense, for the present study, the maximum dissipation (10%) takes place at 130 K, which is 15 K below T_W. To mention the case of SG nanoparticles (with disordered surface spins), the larger the nanoparticle, the closer the drop to T_W, being even found at T_W for the large 40 nm $GdCu_2$ nanoparticles, but even, for the Super Spin Glass (approx. 8 nm size) ones [41]. The present result suggests that the correlations building up the GP clusters are shorter with respect to those of other more conventional SG. The χ'' (t) dependence included in Fig. 5(b) at T_W = 145 K also evidences the expected slow dynamics ascribed to metastable non equilibrium states. There, the displayed relaxation measured at 145 K is well-fitted following an asymptotic power-law decay ($\chi'' \propto t^{-d}$) with d = 0.04. This value is remarkably smaller compared to d = 0.2 obtained close to T_C in re-entrant FM $CdCr_{2x}In_{2-2x}S_4$ [54], accounting for a slower dynamics, which is interpreted as if the non equilibrium state within the Griffiths regime was more robust than in re-entrant FM (*i.e.*, meaning that the FM correlations lock in the SG relaxation). The relaxation in the present $Tb_{4.925}La_{0.075}Si_2Ge_2$ takes place at similar pace than that ascribed to the surface spin glass state of $NdCu_2$ or $GdCu_2$ superantiferromagnetic nanoparticles [41,51]. Compared to $Tb_5Si_2Ge_2$, the presence of non magnetic La ions enhance the inherent out-of-equilibrium dynamics of the GP, as the La ions act as a source of magnetic disorder.

Moving now to 90 K, *i.e.*, below but still close to T_C, memory effects are again observed in Fig. 5(a), although remarkably smaller compared to those obtained at 145 K. In this sense, the SJ = 0.4 at 88 K, 5% downwards the T_W. The $\chi''(t)$ data in Fig. 5(b) also account for a decay (ageing) towards an asymptotic stationary susceptibility, $\chi'' \propto t^{(-0.2)}$, a value that agrees very well with that of re-entrant FM $CdCr_{2x}In_{2-2x}S_4$ [54], and remarkably larger with respect to the one of 0.04 ascribed to the GP. The observation of time-dependent $\chi''(t)$ phenomena within the long-range FM state has been ascribed to the domain wall configuration [54–57]. More precisely, the frustration leading to ageing phenomena arises from the competition between the magnetic coupling energy (FM RKKY favours smooth interfaces) and the pinning energy (disorder favours rough interfaces) [54]. Note that here, the building up process of the long-range FM state in this compound stems from a coalescence of magnetic clusters. It is then

not staggering to infer that such FM order is somewhat formed by a collection of domains in our case (most likely less defined than a truly conventional ferromagnet). The frustrated magnetic interactions are, in our case, weaker with respect to those ascribed to spin glasses. Therefore, our interpretation correlates well with the observation that the relaxation takes place at faster pace in the present situation than that of canonical SG [38,53] and/or the GP of the present sample shown above.

We have also tried to probe ageing and/or memory effect phenomena within the region where FM correlations among GP clusters are settled. To do so, we have selected a temperature value of 116 K, well-below T_{G^*}, the value that marks the onset of these medium-range FM correlations. Remarkably, no memory effects are observed in Fig. 5(a), and the relaxation of the magnetization displayed in Fig. 5(b) linearly drops at a fast pace. This dynamics is somehow surprising, since, additional to the GP, a Cluster-Spin Glass (CSG) state flourishes at 140 K, being both phases expected to evidence out-of-equilibrium dynamics. Considering this, the lack of ageing and memory effects clearly indicates the strength of FM correlations among the clusters, which are already dominating the global magnetic response of the system below 125 K [34]. This leads the system to an intermediate situation, where clusters ascribed to the Griffiths regime are more and more FM aligned, but still the long-range FM state is not settled. As a result, the dynamic response of the system changes completely, and, although the Griffiths and the spin glass clusters shall account for non equilibrium phenomena, the inter-cluster FM interactions are actually strong and hamper the observation of the subtle fingerprints ascribed to these out-of-equilibrium phenomena.

3.3. Small-angle neutron scattering

A microscopic confirmation of the presence of magnetic clusters is a must at this point. Fig. 6(a) displays the magnetic SANS intensity *I(q)* as a function of the momentum transfer q at zero applied magnetic field (H = 0) and at six specific temperatures below T_G (T = 100, 135, 140, 150, 155, and 180 K); these are representative of the various important magnetic regimes in the system. The temperature dependence of the magnetic correlation length l_C is displayed in Fig. 6(b). This quantity was determined from the magnetic correlation function *C(r)* (see inset in Fig. 6(b)), computed from the *I(q)* data via direct Fourier transformation [58,59]. The quantity l_C may be seen as a characteristic length scale that reflects the temperature-dependent transitions expected within the GP scenario. According to the sketched phase diagram in Fig. (1(a)), all the measured temperatures included in Figs. 6(a) and 6(b) fall into the GP-like regime.

The zero-field magnetic SANS intensity *I(q)* in Fig. 6(a) exhibits a large temperature dependence, *i.e.*, between 180 K and 100 K, the signal changes by about four orders of magnitude. The *I(q)* curves between 180 K and 135 K feature essentially the same (or a very similar) dependency on the momentum transfer q, corresponding to a correlation length l_C (Fig. 6(b)) that is relatively small (between about 1–5 nm), close to the resolution limit of the conventional SANS technique. When decreasing the temperature to 100 K (ferromagnetic regime), an increase in *I(q)* is observed that goes along with a change in the curvature of *I(q)* and a large increase in l_C to about 17 nm. While not providing a definite proof, the temperature evolution of the correlation length qualitatively reflects the formation of a GP phase out of the paramagnetic regime and the concomitant gradual build-up of clusters and ferromagnetic correlations at low temperatures. The observed temperature variation is also reflected in a change of the asymptotic power-law exponent in $I(q) \sim q^{-m}$: while the data at the higher temperatures are approximately described by $m = 2$, which is indicative of an Ornstein-Zernicke correlation function, the *I(q)* data set at 100 K exhibits an increased exponent approaching $m = 4$, suggesting the presence of ferromagnetic correlations.

It is helpful now to suggest some qualitative pictures of the magnetic states throughout the temperature variation in the region of interest. This is obviously a simplified view but it becomes visually convenient and it is possible apply the concept to other GP systems, including magnetic disorder. In this sense, the schematic diagrams of the magnetic state depending on the temperature range in the $Tb_{4.925}La_{0.075}Si_2Ge_2$ are represented in Fig. 7. At $T > T_G$ (185 K), all the magnetic moments are randomly arranged and the system is in the (conventional) PM state. When temperature decreases below T_G, GP clusters generate some weak ferromagnetic correlations. These correlations are evidenced and quantified by the increase of l_C (Fig. 6(b)) as cooling down. With a further decrease of temperature to 155 K (T_{G^*}), the ferromagnetic clusters embedded in the paramagnetic matrix become smaller (as detected in M(H)) but the correlations keep on growing from nearly single-cluster size (2 nm) towards l_C to about 4 nm at the freezing temperature (140 K as seen by χ_{AC}) and up to about 18 nm as T_C is approached. It is worth mentioning that these correlations among clusters (evaluated as an increasing value of l_C while cooling down) have been discussed in ensembles of well-defined magnetic nanoparticles. In these, the clusters (particles) are sharply defined compared to GP-like systems. However, the physics and interactions behave similarly, that is, dipole-coupled interactions build up being the reason for these correlations [60]. In particular, in the newly-synthesized nanoflowers, supraferromagnetic correlations have been revealed by polarized SANS [61]. Finally, below T_C(100 K) long-range ferromagnetic state sets in, and conventional magnetic domains are formed. The most relevant (and attractive from the physics standpoint) region in this compound is that around 150 K. At such a temperature (and close by) the Cluster-Spin Glass state is coexisting with GP, being a novel state in magnetic spin arrangements [34]. There, when a magnetic field (even small) is applied, GP is nearly destroyed, not surprisingly as the cluster size is small, and the number of clusters (which will become frozen at T_F) is increased.

The commented magnetic clustering process mirrors systems of ferromagnetic re-entrant spin glasses witnessing the universality and the attraction of the GP state. We firstly note the case of an alloy on the verge of long-range ferromagnetism with magnetic clusters [62] such as $Lu(Fe_{0.5}Al_{0.5})_2$, of metallic nature. There, it turned out that the dilution of the parent alloy RFe_2 by including Lu/Al into a cubic or hexagonal lattice promotes a magnetic arrangement landscape similar to that of $(TbLa)Si_2Ge_2$. The region where clusters form is a metastable regime, similar to structural glasses, and is characterized in the present work by the magnetic history (ageing analysis).

The metastability could be easily modified if the magnetic history of the compound is altered. Indeed, the developing process on cooling should be dependent on the same magnetic ingredients in both $Lu(FeAl)_2$ and $(TbLa)Si_2Ge_2$ systems, more precisely the competition between the exchange and the magnetic (random) anisotropy. In the latter GMC compound, the random inclusion of nonmagnetic La atoms in the lattice is in the origin of the Cluster-Spin Glass at the nanoscale. This arises from the perturbation in the Tb/La R*2* site occupancy within the *Pnma* structure [34], provoking the frustration required for the existence of magnetic disorder. This magnetic disorder is then modified with the advent of larger magnetic clusters (in the CSG state) and there, the pure magnetic clusters with overall FM coupling, become randomly oriented enhancing the magnetic disorder.

Another *mirror* system in metallic state is $CeNi_{1-x}Cu_x$ (orthorhombic structure). In connection to strongly correlated electron systems (SCES) following well-known Doniach's diagram, this system was thoroughly studied to understand the presence of magnetic clusters above T_C. While there is no direct mention of GP, the mechanisms driving the evolution towards cluster percolation (on the scale of ~ 2 nm) exhibit a pattern similar to that observed in $(TbLa)Si_2Ge_2$, albeit occurring at much lower temperatures (T < 5K) [63]. In this sense, theoretical phase diagrams to explain the existence of clusters above T_C, truly resembling the behaviour of our compound have been reported by S. G Magalhaes et al. [64]. A SG phase was predicted above the ferromagnetic order.

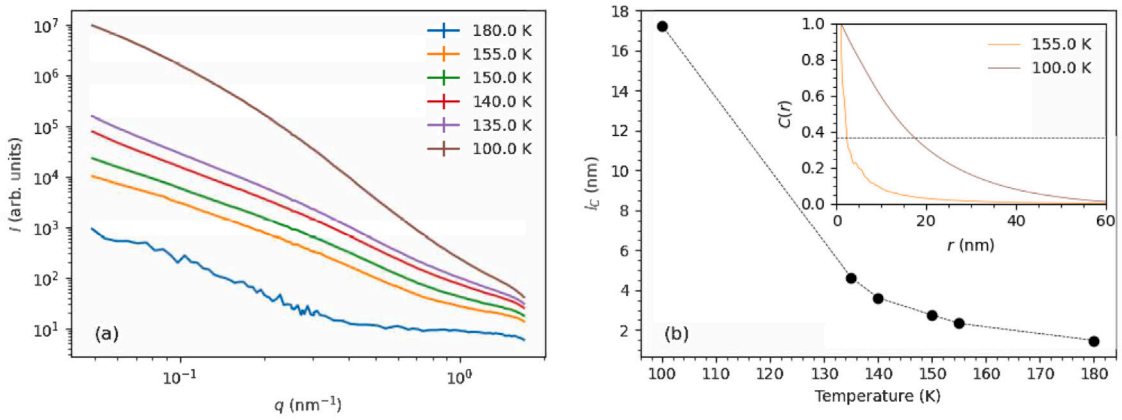

Fig. 6. (Colour online) (a) Magnetic SANS intensity $I(q)$ as a function of the momentum transfer q (log–log scale) for $Tb_{4.925}La_{0.075}Si_2Ge_2$ at selected temperatures between 100 K (brown line) and 180 K (blue line) and at zero applied magnetic field. Values for the temperature are indicated in the insets and decrease from bottom to top. (b) Temperature variation of the magnetic correlation length l_C of $Tb_{4.925}La_{0.075}Si_2Ge_2$ determined from the computed correlation function $C(r)$. The inset shows the normalized magnetic correlation function $C(r)$ of $Tb_{4.925}La_{0.075}Si_2Ge_2$ for two representative temperatures within the GP: 155 K (orange line) and 100 K (brown line). The correlation functions were numerically computed by a direct Fourier transformation using the data shown in (a). Dotted horizontal line in the inset: $C(r) = exp(-1)$ used for determining l_C.

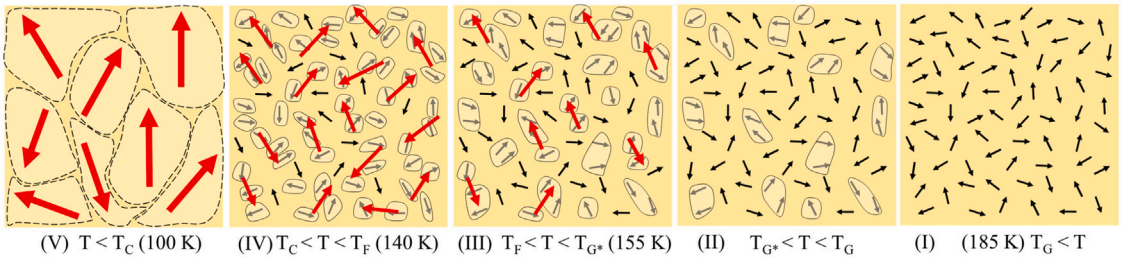

Fig. 7. (Colour online) Schematic diagrams of the evolution of the magnetic arrangement from the conventional paramagnetic state to GP and CSG, and then to FM (with domains), while decreasing temperature (I) PM, (II) GP in the PM, (III) GP clusters with FM, (IV) CSG and GP clusters and (V) FM with conventional ferromagnetic domains. In this simplified pictorial view, the clusters are detailed as moments encircled by a line. The red arrows depict short range FM correlations building up when gradually intercluster interactions and exchange overcomes local anisotropy. The ferromagnetic domains are represented as regions delineated by dashed lines.

It is true that they were dealing with a Kondo Interaction (which is non existent in $(TbLa)Si_2Ge_2$) on top of randomness of the exchange interaction (a basic ingredient for the appearance of SG) plus the random magnetic local fields (anisotropy). An extension of such an approach might be appropriate to tackle our findings theoretically, including the presence of clusters in connection to Magnetocaloric compounds are already developed. Effectively, their triangular Ising spin model predicts an increase of the magnetocaloric effect [65].

In the same (*mirror*) direction, several colossal magnetoresistance (CMR) systems based on manganite oxides and similar materials could also be considered. These have been studied in depth since a couple of decades. For example, in $LaPbMnFeO_3$ using SANS, the report deals with the analysis of the total signal encompassing both nuclear and magnetic contributions [66]. The nuclear component was then modelled by a collection of spheres with a standard form factor combined with a Percus–Yevick arrangement, while the magnetic contribution was described using a sum of a Lorentzian and Lorentzian-squared form. The fitting procedure yielded an average radius of the magnetic cluster size in the vicinity of 4 nm. Here, the weaker (*i.e.*, less intense and more fragile) GP arrangement is better quantified by performing a subtraction of the paramagnetic signal and then naturally extracting an unambiguous magnetic SANS $I(q)$. This procedure results in a precise definition of the magnetic moment-moment correlations procuring us the values of l_C (see Fig. 6(b)). In fact, in the archetypal CMR compound $LaCaMnO_3$, the presence of magnetic clusters with an average size of 1.2 nm was also detected. Notably, these clusters were observed to grow in size upon the application of a magnetic field. As has been extensively studied, such magnetic clustering forms the foundation for understanding the CMR effect [67]. Indeed, this finding may render useful magnetoresistance measurements of the present $(TbLa)Si_2Ge_2$ compound in the thermal region of interest ($100 < T \leq 190$ K). A very recent step forward in the GP analyses has been reported in other very different magnetic compounds to ours, namely Heusler (Ni_2MnSb) alloys [26], - non magnetic elements with a ferromagnetic response. In their report, Tian et al. showcase the same magnetic panorama as the one presented here, and the origin of their magnetic findings is connected to local lattice distortions (cubic *Fm-3m*) in GP at high temperatures ($329 \text{ K} < T < 458$ K). Unfortunately, it is not straightforward to obtain either HRTEM and/or high-resolution X-ray diffraction data (needed in the thermal region of interest) to confirm such subtleties for $T < 180$ K in $Tb_{4.925}La_{0.075}Si_2Ge_2$. It is then clear that the analysis of the GP in connection of CSG constitutes a challenging task which gathers steady attention.

To finish off, returning to the basics of the intrinsic approximations of the GP, Bray [10] theoretically discusses that the relaxation due to Griffiths singularities might exhibit a non-exponential behaviour. This feature is detected here at $T = 116$ K, just above T_C (see Fig. 5(b)). This positive result should be interpreted cautiously, as the relaxation landscape associated with the choice of waiting temperature and time

conditions can be experimentally challenging. Moreover, the presence of spin correlations detected via SANS may alter such a theoretical idealization. It has been proposed that the spin-spin autocorrelation function exhibits a stretched exponential behaviour within the Griffiths phase. While evaluating this directly poses challenges, neutron spin echo (NSE) experiments offer a potential pathway. In such experiments, the scattering function (spin autocorrelation function) of the *S(q,t)* structure factor is analysed over time. This approach could provide microscopic insights into the shape of the relaxation rate, as demonstrated in canonical spin glasses like CuMn (5%)—dilute spins in a metallic matrix [68]—or in slightly larger entities with well-defined boundaries, such as the archetypal 4.6(1) nm Fe(Cu) nanoparticles [69]. Interestingly, in AuFe, a classical metallic Heisenberg SG with local anisotropy, GP where taken into account for T ≈ 2–3 T_F in NSE [70]. It is worth noting that the original work by Griffiths [9] was theoretically developed for an Ising ferromagnet, which is likely not to be the case in our system (or in similar cases). More precisely, the nonlinear susceptibility previously reported in the same compound $Tb_{4.925}La_{0.075}Si_2Ge_2$ [34] indicates that the value for the critical exponent $z\nu = 6.0(1)$ associated with the critical slowing down process above the freezing temperature, aligns with values observed in other clustered systems that more closely behave as an isotropic Heisenberg spin glass [71].

4. Conclusions

The $Tb_{5-x}La_xSi_2Ge_2$ family of compounds constitutes a phenomenal playground to investigate disordered structure with some degree of magnetic clustering. Unlike the more extensively studied magnetic glassy metals, this clustering occurs at temperatures higher than the ferromagnetic state. By selecting a minimum amount of La doping (x = 0.075) a novel state of magnetic arrangement appears, where a CSG is formed, with a freezing transition. This state was reported previously at a macroscopic level but the spin dynamics and the intimate microscopic state at the nanoscale had not been investigated. Here, we have shown that the dynamics of such clustered state is affected by the progressive coupling among CSG and GP phases, towards a FM order. Furthermore, memory effects and ageing phenomena are revealed within the GP phase. Small-angle neutron scattering provides evidence at the nanoscale of the evolution of the magnetic clusters towards T_C, in which a long-range ferromagnetic order is established with the presence of magnetic domains.

In summary, there is evidence for a spin structure that somewhat mirrors- in-temperature (in present data, the magnetic inhomogeneities are found above T_C) that of the better-known ferromagnetic re-entrant spin glasses (there, the magnetic inhomogeneities are found below T_C). Surely, future micromagnetic calculations could deliver further evidence about the evolution of GP clusters. In addition, an interesting future is envisaged for this special compound (and maybe slight variations in x) using polarized SANS combined with micromagnetic simulations. It would also be desirable to follow the temperature evolution of the magnetic SANS signal for certain q-values. The complexity, which is a present driving force for the research in magnetism, is the attraction of this system, which in turn technologically stands out as a promising magnetocaloric material. Future SANS experiments that extend to smaller momentum transfers and in the presence of an applied magnetic field might provide a more detailed picture of the evolving correlation length. Likewise, neutron spin-echo spectroscopy will yield valuable information on the characteristic time scales describing the GP scenario.

CRediT authorship contribution statement

N. Marcano: Writing – review & editing, Writing – original draft, Methodology, Investigation, Conceptualization. **E.M. Jefremovas:** Writing – review & editing, Methodology, Investigation, Formal analysis. **I. Titov:** Writing – review & editing, Formal analysis, Conceptualization. **A. Michels:** Writing – review & editing, Methodology, Investigation, Formal analysis. **N.J. Steinke:** Investigation. **J.H. Belo:** Writing – review & editing, Resources, Methodology. **J.P. Araújo:** Writing – review & editing, Resources, Methodology. **P.A. Algarabel:** Writing – review & editing, Resources, Funding acquisition. **L. Fernández Barquín:** Writing – review & editing, Supervision, Resources, Methodology, Funding acquisition, Conceptualization.

Declaration of competing interest

The authors declare the following financial interests/personal relationships which may be considered as potential competing interests: Luis Fernandez Barquin reports financial support was provided by Spain Ministry of Science and Innovation. P A Algarabel reports financial support was provided by Spain Ministry of Science and Innovation. If there are other authors, they declare that they have no known competing financial interests or personal relationships that could have appeared to influence the work reported in this paper.

Acknowledgements

This research was funded by Spanish MCIN/AEI/10.13039/501100011033 (grant number PID2020-112914RB-100 and PID2023-146448OB-C22) and the Aragón Regional government (grant number E28-20R). This project has received funding from the European Union's Horizon Europe research and innovation program through the European Innovation Council under the grant agreement No 101161135 - MAGCCINE. JH Belo acknowledges PTDC/EMETED/3099/2020, UIDP/04968/2020 Programático, NECL-NORTE 010145-FEDER022096, UIDB/04968/2020, CERN/FISTEC/0003/2019 and FCT for his contract DL57/2016 reference SFRH-BPD8730/2012. EMJ thanks Postdoc grant (von Humboldt). The authors acknowledge the technical assistance of the ILL staff.

References

[1] G. Parisi, Spin glasses and fragile glasses: Statics, dynamics and complexity, Proc. Natl. Acad. Sci. USA 103 (2006) 7948;
R Nuzzo, Profile of giorgio parisi, Proc. Natl. Acad. Sci. U.S.A.1 03 (2006) 7945.
[2] H. Kawamura, T. Taniguchi, Spin glasses, in: K H J Buschow (Ed.), in: Handbook of Magnetic Materials, vol. 24, Elsevier, Amsterdam, 2015, p. 1.
[3] L.P. Lévi, Critical dynamics of metallic spin glasses, Phys. Rev. B. 38 (1988) 4963.
[4] D.S. Fisher, D.A. Huse, Nonequilibrium dynamics of spin glasses, Phys. Rev. B. 38 (1988) 373.
[5] V.K. Anand, D.T. Adroja, A.D. Hillier, Ferromagnetic cluster spin-glass behavior in $PrRhSn_3$, Phys. Rev. B. 85 (2012) 014418.
[6] J.A. Mydosh, Spin glasses: redux: an updated experimental/materials survey, Rep. Progr. Phys. 78 (2015) 052501.
[7] P. Bag, P.R. Baral, R. Nath, Cluster spin-glass behavior and memory effect in $Cr_{0.5}Fe_{0.5}Ga$, Phys. Rev. B. 98 (2018) 144436.
[8] E.M. Jefremovas, et al., Investigating the size and microstrain influence in the magnetic order/disorder state of $GdCu_2$ nanoparticles, Nanomaterials 10 (2020) 2148.
[9] R.B. Griffiths, Nonanalytic behavior above the critical point in a random ising ferromagnet, Phys. Rev. Lett. 23 (1969) 17.
[10] A.J. Bray, Nature of the Griffiths phase, Phys. Rev. Lett. 59 (1987) 586.
[11] A.H. Castro Neto, G. Castilla, B.A. Jones, Non-Fermi liquid behavior and Griffiths phase in f-Electron compounds, Phys. Rev. Lett. 81 (1998) 3531.
[12] J. Deisenhofer, et al., Observation of a Griffiths phase in paramagnetic $La_{1-x}Sr_xMnO_3$, Phys. Rev. Lett. 95 (2005) 257202.
[13] S. Zhou, Y. Guo, J. Zhao, L. He, L. Shi, Size-induced Griffiths phase and second-order ferromagnetic transition in $Sm_{0.5}Sr_{0.5}MnO_3$ nanoparticles, J. Phys. Chem. C 115 (2011) 1535.
[14] S.K. Giri, S. Yusuf, M.D. Mukadam, T.K. Nath, Emergence of Griffiths phase and glassy mixed phase in $Sm_{0.5}Ca_{0.5}MnO_3$ nanomanganites, J. Alloys Compd. 591 (2014) 181.
[15] S. Saha, A. Dutta, S. Gupta, S. Bandyopadhyay, I. Das, Origin of the Griffiths phase and correlation with the magnetic phase transition in the nanocrystalline manganite $La_{0.4}(Ca_{0.5}sr_{0.5})_{0.6}MnO_3$, Phys. Rev. B. 105 (2022) 214407.
[16] R. Lu, et al., Evidence for a Griffiths Phase to Cluster Spin Glass Transition in the $La_{2/3}Sr_{1/3}(Mn_{1-3x}Al_{2x}Ti_x)O_3$ System, Adv. Sci. (2024) 2408517.

[17] M.B. Salamon, P. Lin, S.H. Chun, Colossal magnetoresistance is a Griffiths singularity, Phys. Rev. Lett. 88 (2002) 197203.
[18] S. Guo, D.P. Young, R.T. Macaluso, D.A. Browne, N.L. Henderson, J.Y. Chan, L.L. Henry, J.F. DiTusa, Discovery of the Griffiths phase in the itinerant magnetic semiconductor $fe_{1-x}Co_xs_2$, Phys. Rev. Lett. 100 (2008) 017209.
[19] M. Brando, D. Belitz, F.M. Grosche, T.R. Kirkpatrick, Metallic quantum ferromagnets, Rev. Modern Phys. 88 (2016) 025006.
[20] Z. Wang, Y. Liu, Ch. Ji, J. Wang, Quantum phase transitions in two-dimensional superconductors: a review on recent experimental progress, Rep. Progr. Phys. 87 (2024) 014502.
[21] R. Revathy, N. Kalarikkal, M.R. Varma, K.P. Surendran, Exchange-spring mechanism and Griffiths-like phase in room-temperature magnetoelectric Ni–$BaTiO_3$ composites, Mater. Adv. 2 (2021) 4702.
[22] R. Revathy, N. Kalarikkal, M.R. Varma, K.P. Surendran, Exotic magnetic properties and enhanced magnetoelectric coupling in Fe_3O_4-$BaTiO_3$ heterostructures, J. Alloys Compd. 889 (2021) 161667.
[23] K. Yadav, M.K. Sharma, S. Singh, K. Mukherjee, Exotic magnetic behaviour and evidence of cluster glass and Griffiths like phase in Heusler alloys $Fe_{2-x}Mn_xCrAl(0 \leq x \leq 1$, Sci Rep. 9 (2019) 15888.
[24] S. Chatterjee, S. Giri, S. Majumdar, P. Duta, P. Singha, A. Banerjee, Observation of Griffiths-like phase in the quaternary Heusler compound NiFeTiSn, J. Phys.: Condens. Matter. 34 (2022) 295803.
[25] J. Nag, P.C. Sreeparvathy, R. Venkatesh, P.D. Badu, K.G. Suresh, A. Alam, Nontrivial topological features and griffith's-phase behavior in CrFeVGa probed by experiment and theory, Phys. Rev. Appl. 19 (2023) 044071.
[26] F. Tian, Q. Zhao, J. Guo, Y. Zhang, M. Fang, T. Chang, Z. Dai, C. Zhou, K. Cao, S. Yang, Griffiths phase arising from local lattice distortion and spin glass above the curie temperature in Ni_2MnSb polycrystalline Heusler alloy, Phys. Rev. B. 109 (2024) 224405.
[27] C. Magén, P.A. Algarabel, L. Morellón, J.P. Araújo, C. Ritter, M.R. Ibarra, A.M. Pereira, J.B. Sousa, Observation of a Griffiths-like phase in the magnetocaloric compound $Tb_5Si_2Ge_2$, Phys. Rev. Lett. 96 (2006) 167201.
[28] A.M. Pereira, L. Morellón, C. Magén, J. Ventura, P.A. Algarabel, M.R. Ibarra, J.B. Sousa, J.P. Araújo, Griffiths-like phase of magnetocaloric $R_5(Si_xGe_{1-x})_4$ (R=Gd, Tb, Dy, and Ho), Phys. Rev. B. 82 (2010) 172406.
[29] Y. Mudryk, V.K. Pecharsky, K.A. Gschneidner Jr., R5t4 compounds: An extraordinary versatile model system for the solid state science, (Handbook on the Physics and Chemistry of Rare Earths, vol. 44, Elsevier, New York, 2014, p. 283,
[30] J.H. Belo, A.L. Pires, I.T. Gomes, V. Andrade, J.B. Sousa, R.L. Hadimani, D.C. Jiles, Yang. Ren, X. Zhang, J.P. Araújo, A.M. Pereira, Giant negative thermal expansion at the nanoscale in the multifunctional material $Gd_5(Si, Ge)_4$, Phys. Rev. B. 100 (2019) 134303.
[31] J.Y. Law, V. Franco, Review on magnetocaloric high-entropy alloys: Design and analysis methods, J. Mater. Res. 38 (2023) 37.
[32] W. Choe, V.K. Pecharsky, O.A. Pecharsky, K.A. Gschneidner Jr., V.G. Young, J.G. Miller, Making and Breaking Covalent Bonds across the Magnetic Transition in the Giant Magnetocaloric Material $Gd_5(Si_2Ge_2)$, Phys. Rev. Lett. 84 (2000) 4617.
[33] J.H. Belo, et al., Tailoring the magnetism of $Tb_5Si_2Ge_2$ compounds by La substitution, Phys. Rev. B. 86 (2012) 014403.
[34] N. Marcano, P.A. Algarabel, L. Fernández Barquín, J.P. Araújo, A.M. Pereira, J.H. Belo, C. Magén, L. Morellón, M.R. Ibarra, Cluster-glass dynamics of the Griffiths phase in $Tb_{1-x}La_xSi_2Ge_2$, Phys. Rev. B. 99 (2019) 054419.
[35] J.A. Mydosh, Spin Glasses: An Experimental Introduction Ed Taylor & Francis, CRC Press, London, 1993.
[36] P. Svedlindh, K. Gunnarsson, J.O. Andersson, H.A. Katori, A. A. Ito, Time-dependent ac susceptibility in spin glasses, Phys. Rev. B. 46 (1992) 13867.
[37] P. Nordblad, P. Svedlindh, Experiments on spin glasses, in: A P Young (Ed.), Spin Glasses and Random Fields, in: Series on directions in Condensed Matter Physics, vol. 12, World Scientific, Singapore, 1998, p. 1.
[38] K. Jonason, E. Vincent, J. Hammann, J.P. Bouchaud, P. Nordblad, Memory and chaos effects in spin glasses, Phys. Rev. Lett. 81 (1998) 3243.
[39] P. Jönsson, M. Hansen, P. Svedlindh, P. Nordblad, Memory effects in an interacting magnetic nano-particle sample, Phys. B 284 (2000) 1754.
[40] D. Joshi, G. Gebresenbut, C.P. Gómez, R. Mathieu, Memory and rejuvenation in a quasicrystal, EPL 132 (2020) 27002.
[41] E.M. Jefremovas, P. Svedlindh, L. Fernández Barquín, Dual disorder-driven magnetic dynamics in $GdCu_2$ superantiferromagnetic nanoparticles, J Nanopart Res. 24 (2022) 194.
[42] J.L. Garlea, C.Y. Zarestky, L.L. Jones, D.L. Lin, T.A. Schlagel, A.O. Lograsso, V.K. Tsokol, K.A. Pecharsky, V.O. Gschneidner Jr., C. Stassis, Neutron diffraction studies of the magnetoelastic compounds $Tb_5Si_xGe_{4-x}$ (x=2.2 and 2.5), Phys. Rev. B. 72 (2005) 104431.
[43] J.P. Araújo, et al., Transport and magnetic study of the spin reorientation transition in the $Tb_5(Si_{0.5}Ge_{0.5})_4$ magnetocaloric compound, J. Phys.: Condens. Matter. 17 (2005) 4941.
[44] C. Ritter, L. Morellón, P.A. Algarabel, C. Magén, M.R. Ibarra, Magnetic and structural phase diagram of $Tb_5(Si_xGe_{1-x})_4$, Phys. Rev. B. 65 (2002) 094405.
[45] R. Saha, V. Srinivas, T.V. Chandrasekhar Rao, Evolution of ferromagneticlike order in $Fe_2V_{1-x}Cr_xAl$ Heusler alloys, Phys. Rev. B. 79 (2009) 174423.
[46] W. Akram, M. de h Óra, M. Bansal, R. Mukhopadhyay, J. MacManus-Driscoll, T. Maity, Table-like magnetocaloric effect due to field-induced inter-cluster interactions in $Eu_{0.5}Sr_{0.5}MnO_3$–$EuMnO_3$ composites, J. Phys. D: Appl. Phys. 57 (2024) 055301.
[47] P. Anil Kumar, A. Nag, R. Mathieu, R. Das, S. Ray, P. Nordblad, A. Hossain, D. Cherian, D. Alba Venero, L. Debeer-Schmitt, O. Karis, D.D. Sarma, Magnetic polarons and spin-glass behavior in insulating $la_{1-x}sr_xcoo_3$ (x=0.125 and 0.15), Phys. Rev. Res. 2 (2020) 043344.
[48] V.K. Pecharsky, K.A. Gschneidner Jr., Phase relationships and crystallography in the pseudobinary system Gd_5Si_4-Gd_5Ge_4, J. Alloys Compd. 260 (1997) 98.
[49] C.P. Bean, J.D. Livingston, Superparamagnetism, J. Appl. Phys. 30 (1959) S120.
[50] B. Roy, S. Das, Magnetic cluster glass behavior and grain boundary effect in $Nd_{0.7}Ba_{0.3}MnO_3$ nanoparticles, J. Appl. Phys. 104 (2008) 103915.
[51] E.M. Jefremovas, P. Svedlindh, F. Damay, D. Alba Venero, A. Michels, J.A. Blanco, L. Fernández Barquín, Magnetic order and disorder environments in superantiferromagnetic $NdCu_2$ nanoparticles, Sci Rep. 12 (2022) 9733.
[52] E.M. Jefremovas, M. de la Fuente Rodríguez, D. Alba Venero, C. Echevarría-Bonet, P. Bender, B. Fåk, J.A. Blanco, L. Fernández Barquín, Magnetic super-structure and active surface role in the onset of magnetic excitons revealed in $TbCu_2$ nanoparticles, Commun Mater 4 (2023) 56.
[53] C. Djurberg, K. Jonason, P. Nordblad, Magnetic relaxation phenomena in a CuMn spin glass, Eur. Phys. J. B. 10 (1999) 15.
[54] V. Dupuis, E. Vincent, M. Alba, J. Hammann, Aging, Rejuvenation and memory effects in re-entrant ferromagnets, Eur. Phys. J. B. 29 (2002) 19.
[55] E. Vincent, V. Dupuis, M. Alba, J. Hammann, J.P. Bouchaud, Aging phenomena in spin-glass and ferromagnetic phases: Domain growth and wall dynamics, Europhys. Lett. 50 (2000) 674.
[56] K. Jonason, J. Mattsson, P. Nordblad, Chaos in the ferromagnetic phase of a reentrant ferromagnet, Phys. Rev. Lett. 77 (1996) 2562.
[57] R. Mathieu, P. Nordblad, D.H.N. Nam, N.X. Phuc, N.V. Khiem, Short-range ferromagnetism and spin-glass state in $Y_{0.7}Ca_{0.3}MnO_3$, Phys. Rev. B. 63 (2001) 174405.
[58] J. Weissmuller, A. Michels, D. Michels, A. Wiedenmann, III. C. E. Krill, H.M. Sauer, R. Birringer, Spin structure of nanocrystalline terbium, Phys. Rev. B. 69 (2004) 054402.
[59] D. Mettus, A. Michels, Small-angle neutron scattering correlation functions of bulk magnetic materials, J. Appl. Crystallogr. 48 (2015) 1437.
[60] P. Bender, E. Wetterskog, D. Honecker, J. Fock, C. Frandsen, C. Moerland, L.K. Bogart, O. Posth, W. Szczerba, H. Gavilán, R. Costo, M.T. Fernández-Díaz, D. González-Alonso, L. Fernández Barquín, C. Johansson, Dipolar-coupled moment correlations in clusters of magnetic nanoparticles, Phys. Rev. B. 98 (2018) 224420.
[61] P. Bender, D. Honecker, L. Fernández Barquín, Supraferromagnetic correlations in clusters of magnetic nanoflowers, App. Phys. Lett. 115 (2019) 132406.
[62] C. Piquer, L. Fernández Barquín, J. Chaboy, D. Alba-Venero, M.A. Laguna-Marco, R. Boada, I. Puente-Orench, Magnetic clusters on the verge of long range ferromagnetism in $Lu(Fe_{0.75}Al_{0.25})_2$ and $Lu(Fe_{0.50}Al_{0.50})_2$ alloys, J. Alloys Compd. 695 (2017) 704.
[63] N. Marcano, J.C. Gómez Sal, J.I. Espeso, J.M. De Teresa, P.A. Algarabel, C. Paulsen, J.R. Iglesias, Mesoscopic Magnetic States in Metalllic Alloys with Strong Electronic Correlations: A Percolative Scenario for $CeNi_{1-x}Cu_x$, Phys. Rev. Lett. 98 (2007) 166496.
[64] S.G. Magalhaes, F.M. Zimmer, P.R. Krebs, B. Coqblin, Spin glass and ferromagnetism in disordered cerium compounds, Phys. Rev. B. 74 (2006) 014427.
[65] F.M. Zimmer, R. Mourão, M. Schmidt, M.A. Tumelero, S.G. Magalhaes, Enhancement of the magnetocaloric effect in geometrically frustrated cluster spin glass systems, J. Phys.: Condens. Matter. 35 (2023) 315801.
[66] N. Veglio, F.J. Bermejo, J. Gutiérrez, J.M. Barandiarán, A. Peña, M.A. González, P.P. Romano, C. Mondelli, Experimental evidence of a cluster-glass transition on the colossal magnetoresistance manganite $La_{0.7}Pb_{0.3}(Mn_{0.9}Fe_{0.1})O_3$, Phys. Rev. B. 71 (2005) 212402.
[67] J.M. De Teresa, M.R. Ibarra, P.A. Algarabel, C. Marquina, J. Blasco, J. García, A. del Moral, Z. Arnold, Evidence for magnetic polarons in the magnetoresistive perovskites, Nature 386 (1997) 256.
[68] F. Mezei, A. Murani, Experimental studies of the low-temperature properties of spin glasses, J. Magn. Magn. Mater. 14 (1979) 211.
[69] L.Fernández. Barquín, R. García Calderón, B. Farago, J. Rodríguez-Carvajal, A. Bleloch, D. McComb, R. Chater, Q.A. Pankhurst, Neutron spin echo evidence of mesoscopic spin correlations among Fe(Cu) ferromagnetic nanoparticles in a silver diamagnetic matrix, Phys. Rev. B. 76 (2007) 172404.
[70] C. Pappas, F. Mezei, G. Ehlers, P. Manuel, I.A. Campbell, Dynamic scaling in spin glasses, Phys. Rev. B. 68 (2003) 054431.
[71] Y. Bitla, S.N. Kaul, L. Fernández Barquín, Nonlinear susceptibilities as a probe to unambiguously distinguish between canonical and cluster spin glasses, Phys. Rev. B. 86 (2012) 094405.